ISSN 1392–1320 MATERIALS SCIENCE (MEDŽIAGOTYRA). Vol. 11, No. 3. 2005

The Influence of Pores Distribution Mode on the Stress of Porous Elastomeric Materials in the Case of Large Deformations

Daiva ZELENIAKIENĖ*, Paulius GRIŠKEVIČIUS

Department of Mechanics of Solids, Kaunas University of Technology, Kęstučio 27, LT-44025 Kaunas, Lithuania

Received 27 January 2005; accepted 06 March 2005

Finite element simulations and experimental tests were performed to study the influence of pores distribution mode on the stress of porous elastomeric materials in the case of large deformations. The relationships of principal stress on elongation ratio were obtained as the non-linear dependence of material matrix is described by Mooney-Rivlin equation. The results showed that, the lowest stress forms in such elastomeric material that exhibit the lowest stiffness changes of matrix adjacent zones. If at low elongation ratio values the principal stresses of porous elastomeric polymer material are similar to those of non-porous material with the same mechanical properties as the matrix, at high elongation ratio the principal stresses of porous material are 1.5 – 3 times higher than those of non-porous one. The results of experimental tests provide good agreement with these numerically obtained but the phenomenon of strengthening was observed as the higher stress than true stress at fracture of matrix material appears. This can occur if the pores size is on the order of materials dimensions. Due to this, the strengthening effect would not appear in microporous elastomers.

Keywords: porous elastomer, pores distribution mode, stress, non-linearity, large deformations, microstructural modelling, finite element analysis.

INTRODUCTION

Composites made from various kinds of rubber and elastomer or rubber-like matrix materials have found a wide range of applications in engineering [1]. Nowadays elastomeric materials are used in automobile, spatial, aeronautic, railways or pneumatic industries for assuming links of binding, damping or tightness tasks [2]. The unique feature of elastomer-based composites is that they can exhibit usable ranges of deformations much larger than these of composites with stiffer matrices, such as metals, ceramics, or rigid polymers [1].

The use of porous elastomeric composites is widespread none the less than use of particle-reinforced elastomeric composites. The development and application of porous elastomeric materials is enforced by the continuous demand for lightweight constructions with enhanced mechanical properties [3]. Evidently, pores play a dominant role in the mechanical response of such materials. Depending on the shape, distribution and volume fraction of the pores, the overall properties of the porous elastomeric material will be various.

A separate part of porous materials is formed by foams or so called cellular materials. Although the mechanics of low-density elastomeric foams has been widely investigated [4 – 11], the effects of lower levels of porosity on the mechanical behaviour of elastomeric materials are a subject that has been poorly covered in the literature [12]. Porous elastomers that are not referable to foams usually are fabricated either by the addition of a second phase with a lower density or by the addition of a blowing agent prior to curing [13]. Such porous elastomers typically have bubble (approximate spherical) pores which may be homogeneous or heterogeneous. The pores distribution mode usually has random character, but if some presumptions are made the periodicity of pores distribution can be envisaged.

As it is known, mechanical properties of porous elastomeric materials are governed by the information concerning the detailed topology and morphology of the material microstructure. Two porous media having the same composition of constituents may exhibit quite a different behaviour due to their different microstructures [3]. Two different approaches can be used to study the behaviour of porous material; the macroscopic modelling and the microscopic consideration. Using the first method the medium under consideration is replaced by the overlaying continua and thus all the laws are introduced at the macroscopic level. The second approach is the microscopic modelling and the effect of microstructure on macromechanical behaviour has largely been investigated through micromechanical models.

The micromechanical models usually are defined by representative volume element (RVE). This is the small volume element of the medium considered which should contain all information necessary for the complete description of the medium [3]. The RVE should be large enough to represent the microstructure, without introducing non-existing properties and at the same time it should be small enough to allow efficient computational modelling [14].

The micromechanical modelling of porous elastomeric materials have some advantages over macromechanical this if the more fundamental studies are needed for a better understanding of the deformation behaviour of these advanced materials.

The aim of this investigation was to evaluate the influence of pores distribution mode on the stress of elastomeric materials for the case of large deformations.

*Corresponding author. Tel.: + 370-37-300426; fax: + 370-37-324108.
E-mail address: *Daiva.Zeleniakiene@ktu.lt* (D. Zeleniakienė)

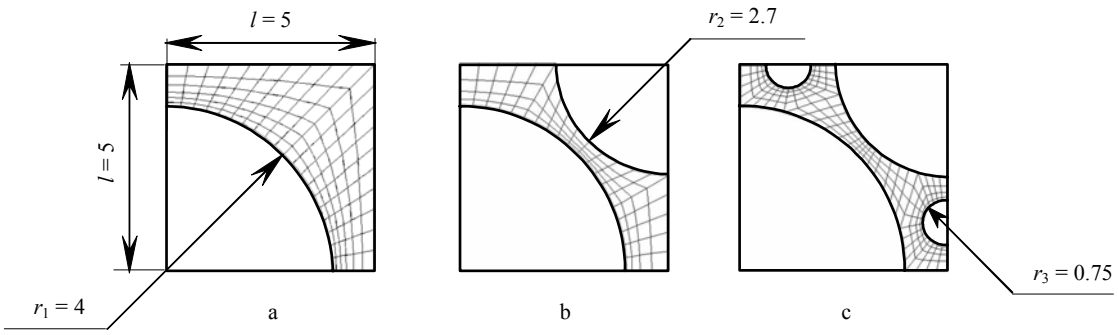

Fig. 1. Unit cells of three investigated models: Model I (a), Model II (b) and Model III (c). Dimensions are in μm

EXPERIMENTAL

The finite element analysis (FEA) was used to identify influence of material pores distribution mode on the stress state of porous elastomeric material. The analysis was performed by finite element code ANSYS. The plane 2D models were made to utilize symmetry and periodicity, assuming that there are no trough-the thickness stresses in the plane. Eight-node quadrilateral PLANE183 (Structural Solid) elements were used. The exact number of elements of each model depends on model type and porosity. In order to obtain the influence of pores distribution mode, three types of plane models, which differ from each other in porosity size, pores distribution mode and stiffness changes of matrix adjacent zones, were investigated [15, 16]. The obtained models are over-simplified representation of porous elastomeric materials structure. Each model was described by a representative volume element. The RVE was constructed from symmetric unit cells, which are the smallest elements of the microstructure. The geometry and finite element mesh of unit cells for three investigated models is presented in Fig. 1. The RVE of each model was obtained from 36 unit cells and the outsider length of square RVE was equal to 30 μm. The porosity was calculated according to this equation:

$$\gamma_p = \frac{\sum_{i=1}^{m}\sum_{j=1}^{n}\frac{\pi d_{ij}^2}{4}}{L^2} = \frac{\frac{\pi n_1 d_1^2}{4}+\frac{\pi n_2 d_2^2}{4}+\frac{\pi n_3 d_3^2}{4}}{L^2} = \frac{\pi(n_1 d_1^2 + n_2 d_2^2 + n_3 d_3^2)}{4L^2} = \frac{\pi}{8L^2}\left(d_1^2 + d_2^2 + 4d_3^2\right), \quad (1)$$

where d_1, d_2, d_3 are the diameters of heterogeneous pores; m is the number of pores sizes, $m = 1, 2, 3$; n_1, n_2, n_3 is the number of pores, respectively of d_1, d_2, d_3. Models I, II and III represent the porous material of porosity value respectively $\gamma_p = 0.5$, $\gamma_p = 0.73$, $\gamma_p = 0.80$.

The boundary conditions on the macroscopic scale were that the upper surface is shear-free with a constant displacement constraint; the bottom surface had constraint on two directions in the point in the symmetry axis of model and this on one direction in other points. Whereas the right and left surfaces were assumed to be stress free.

In order to investigate the nonlinear behaviour of porous elastomeric material, the nonlinear relation between principal stress σ_1 and elongation ratio λ of matrix material butadiene-nitrile rubber SKN-40 was experimentally determined. This rubber was chosen because of the mechanical properties of this good represent the class of elastomeric materials. Standard rectangular shaped specimens were machined using press PKP-10 from the sheet of butadiene-nitrile rubber SKN-40. The tensile tests were run on a tensile testing machine FP10/1 with strain rate 100 mm/min. As the relation between true experimental stress and elongation ratio was determined the equations commonly applied for elastomeric materials were used:
Neo-Hookean [17 – 19]

$$\sigma_1 = G\cdot\left(\lambda^2 - \frac{1}{\lambda}\right), \quad (2)$$

Bartenev-Chazanovich [20]

$$\sigma_1 = A\cdot\left(\lambda - \frac{1}{\sqrt{\lambda}}\right), \quad (3)$$

and Mooney-Rivlin [17, 18]

$$\sigma_1 = \left(2C_1 + \frac{2C_2}{\lambda}\right)\cdot\left(\lambda^2 - \frac{1}{\lambda}\right), \quad (4)$$

where G is the shear modulus, $G = 0.88$ MPa, A, C_1, C_2 are the material constants, $A = 4.55$ MPa, $C_1 = 0.259$ MPa, $C_2 = 0.265$ MPa. Materials constants were determined using code TableCurve2D.

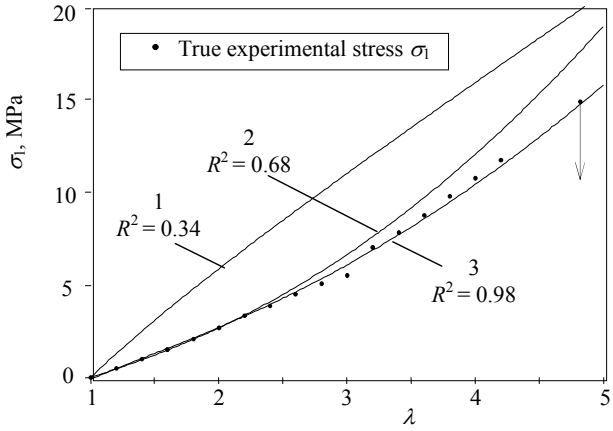

Fig. 2. The relations between true stress σ_1 and elongation ratio λ of butadiene-nitrile SKN-40 rubber: 1 – Bartenev-Chazanovich; 2 – Neo-Hookean; 3 – Mooney-Rivlin; R^2 – determination factor

The experimental results and theoretical ones obtained according to (2), (3) and (4) are presented in Fig. 2. Mooney-Rivlin equation corresponded to the experimental points better than others did, so this equation was chosen for the description of matrix behaviour.

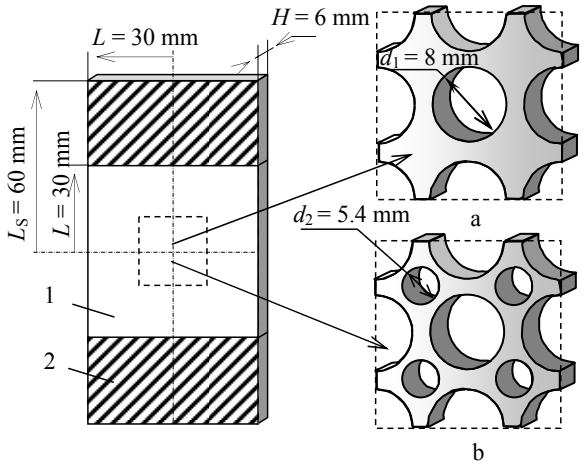

Fig. 3. Specimens from butadiene-nitrile rubber SKN-40: Specimen I (a) and Specimen II (b). 1 – specimen part with cylindrical holes, 2 – monolithic part of specimen for the fixing in the clamps of tensile testing machine

Experimental tests were done to verify the right of obtained numerical results. Proportionally to geometry of investigated numerical Models I and II microstructure the specimens from butadiene-nitrile rubber SKN-40 sheet were machined (Fig. 3). Specimen I and Specimen II were run on tensile testing machine FP10/1 with strain rate of 100 mm/min until they were broken. From a tension diagram $F = f(\Delta L)$ and geometry changes the true stress was calculated. The true stress at fracture σ_{fr} and elongation ratio at fracture λ_{fr} of Specimens I and II were obtained, also.

RESULTS AND DISCUSSIONS

The relations between principal stress and elongation ratio of Model I, Model II, Model III and non-porous material are presented in Fig. 4. It seems that, the mode of investigated Models curves is similar to this of matrix material i. e., model without pores, but if these curves are described by Mooney-Rivlin equation, the low determination factor is obtained ($R^2 \approx 0.6 \div 0.7$). The parabola equation was used and the high determination factor ($R^2 \approx 1$) was obtained:

$$\sigma_1 = A + B\lambda + C\lambda^2 , \qquad (5)$$

where A, B, C are the constants: for Model I $A = -4.66$, $B = 2.86$, $C = 1.55$; for Model II $A = -4.37$, $B = 1.66$, $C = 1.83$; for Model III $A = -2.04$, $B = 1.38$, $C = 1.20$.

As the elongation ratio is the same, the stress of Model I is higher than this of Models II, III and non-porous one. In the case of low elongation ratio values e. g. as $\lambda < 1.4$ the stresses of Models II and III are similar to stress of non-porous material and even of less than this. Therefore, in the case of high elongation ratio $\lambda > 1.4$, the stresses of models II and III are several times higher than these of model without pores. The explanation of this is following. For the case of small deformations, the microstrips of Models II and III have varying orientation with respect to loading direction. As deformation proceed, the microstrips of these Models parallel with loading direction and this does not make the high stress. Due to this, the curves of Models II and III have bevel tangents in the beginning of deformation. For the case of large deformations the microstrips of Models II and III are oriented in loading direction and as deformation proceed they go through the tension and no orientation. So the stresses in this case are increasing and the angles of curves tangents are increasing, also.

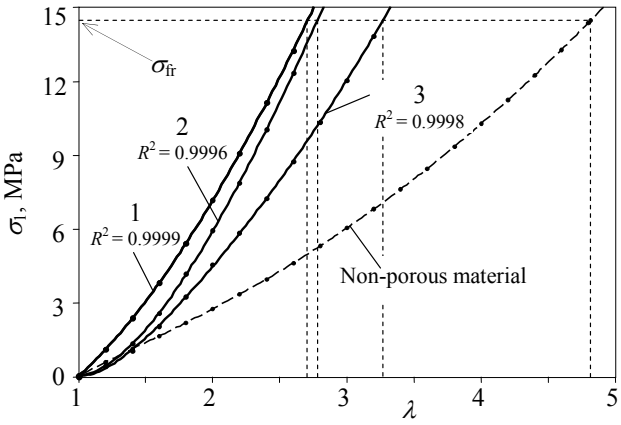

Fig. 4. The relations between principal stress σ_1 and elongation ratio λ of: 1 – Model I, 2 – Model II, 3 – Model III and non-porous material

While all microstrips of Model I are parallel with the loading direction in undeformed stage, yet. The stresses of this model are significantly increasing from the very beginning of deformation process.

The experimental test shows that the true stress at fracture of matrix material is equal to $\sigma_{fr} = 14.4$ MPa. The first of all, the Model I reach this value as the elongation ratio is $\lambda = 2.7$. The next to reach the value of true stress at fracture is the Model II as $\lambda = 2.8$ and last of all the Model III reach this value as $\lambda = 3.3$. The elongation ratio at fracture of investigated Models is respectively 1.8, 1.7 and 1.4 time less than this of non-porous material.

If Models compared together and to non-porous material it is useful to apply the stress concentration factor K_σ. The relationships of stress concentration factor K_σ with respect to elongation ratio λ of Models I, II, III and non-porous material are presented in Fig. 5. The curves of dependences could be described by simply equation:

$$K_\sigma = A + B/\lambda , \qquad (6)$$

where A, B are the constants: for Model I $A = 3.73$, $B = -2.25$; for Model II $A = 4.28$, $B = -4.25$; for Model III $A = 2.92$, $B = -2.72$.

It seems that, the stress concentration factors of Models I, II and III increase as the elongation ratio increase. In the case of low elongation ratio (e. g. $\lambda = 1.2$) the stress concentration factor of Model I is significantly higher than this of Models II, III and nonporous material. The same result was obtained, as the relationship of strains with stress was linear [15]. For large deformations (e. c. $\lambda = 3.5$) the stress concentration factor of Models I and II is about three times higher than this of non-porous

material. While the stress concentration factor of Model III is 2.2 times higher. Therefore in the case of conditionally small deformations the low stress concentration factor is characteristic for Models II and III and the high this for Model I. For large deformations the low stress concentration factor is characteristic only for Model III and the high this for Models I and II. It follows that; if the pores distribution mode of elastomeric material is similar to this of Model III the strength of such material would be significantly higher than this of elastomeric material with pore distribution mode identical to this of Model I.

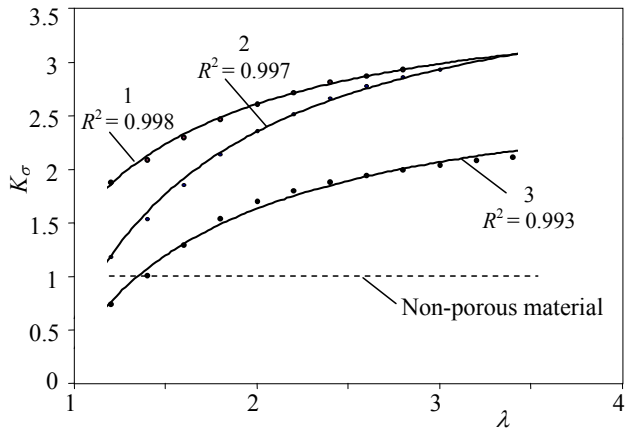

Fig. 5. The relationships of stress concentration factor K_σ with respect to elongation ratio λ of: 1 – Model I, 2 – Model II, 3 – Model III and non-porous material

In order to compare the results obtained by FEA and the experimental these the substantial Specimens I and II from butadiene-nitrile rubber SKN-40 (see Fig. 3) were tested. The experimental and numerical data of the relationships of true principal stress σ_1 with respect to elongation ratio λ of Model I, II and III are presented in Fig. 6. It seems that the experimental points have a good correlation with curves obtained by FEA. But it is evident that true stress at fracture of Specimens I and II is not equal to this of matrix material, i. e. an inequality is valid $\sigma_{fr} < \sigma_{fr}(\mathrm{I}) < \sigma_{fr}\mathrm{II})$ instead of validation of quality $\sigma_{fr} = \sigma_{fr}(\mathrm{I}) = \sigma_{fr}(\mathrm{II})$, where $\sigma_{fr}(\mathrm{I})$ and $\sigma_{fr}(\mathrm{II})$ are the true stress at fracture respectively of Specimen I and II matrix material. Also the experimental elongation rates at fracture of specimens are significantly higher than it was determined by numerical method. The elongation ratio at fracture is equal to 3.4 and 3.9 respectively for specimens I and II. This phenomenon manifested in experimental test could be explained by the effect of large pores and small specimen or in other words by scale factor. The similar phenomenon of strengthening was noticed by Andrews and Gibson [21 – 23]. They investigated the influence of cracks and cell size on tensile strength of aluminium foam with cells of large sizes. Authors observed that the larger the notch and cell size, the more significant the strengthening effect of unnotched zone. They used an equation for the evaluation of strengthening factor. If this equation is applied to case investigated in this study, the strengthening factor (SF) can be written for specimen I as

$$SF = 1 + \frac{2d_1}{L} = 1.53. \tag{7}$$

This theoretical strengthening factor can be compared to experimental this

$$SF = \frac{\sigma_{fr}(I)}{\sigma_{fr}} = 1.62. \tag{8}$$

From equations (7) and (8) it seems that, the difference between the experimental and theoretical strengthening factors is not significant, it reaches just about 5 %. However, the predication that equation is universal and valid in all cases is impossible because the investigations of equation (7) validation is very poor, only one case of porosity value was analysed. Nevertheless, the idea of strengthening effect explanation can be based on theses reasoning.

In the case of specimen II the heterogeneity of pores exists. So the evaluation of pores d_2, not only d_1 is needed. Good congruence of theoretical and experimental results is received if equation (7) is transformed in this way

$$SF = 1 + \frac{2(d_1 + d_2)}{L} = 1.89. \tag{9}$$

Forasmuch the experimental strengthening factor is equal to

$$SF = \frac{\sigma_{fr}(II)}{\sigma_{fr}} = 1.93. \tag{10}$$

So, the difference between experimental and theoretical strengthening factors is only about 2 %. However, it is not good to talk about the universality of equation (9) due to reasons before mentioned.

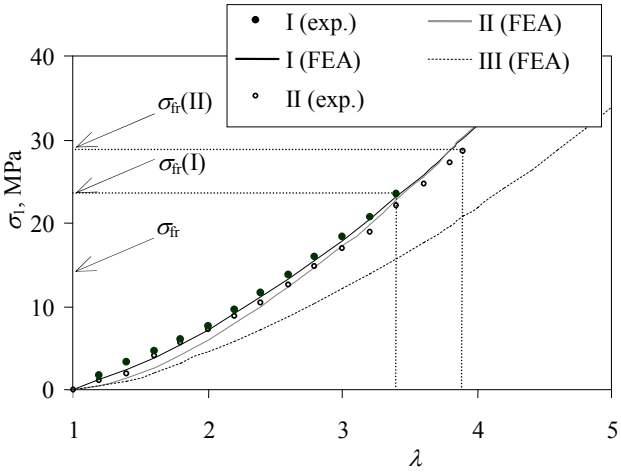

Fig. 6. The experimental and numerical data of the relationships of true principal stress σ_1 with respect to elongation ratio λ of Model I, Model II and Model III

In conformity with a logical mind, the true stress at fracture of specimen III should be increased and the highest of all three specimens, though the experiments of this was not executed due to complex specimen shape. The elongation ratio at fracture of specimen III should be increased, also. Maybe, it could be higher than this of nonporous material.

An ambiguity results were obtained by numerical and experimental methods but they do not negate the veracity of each other. If a microporous elastomer material is under consideration the relation $2d/L$ approximate to zero. Then

the equations (7) and (9) will be equal to one. It means that the strengthening effect will not appear in microporous elastomers. The fracture of these materials may occur, as the stress in microstrips is equal to true stress at fracture of matrix material. Therefore as the size of pores and the dimension of material are of the same order the relation is $2d/L >> 0$ and strengthening effect, i. e. the higher stress than stress at fracture of matrix material, could appear in such elastomers.

CONCLUSIONS

The relationships of porous elastomeric material principal stress on elongation ratio were obtained as the non-linear dependence of material matrix is described by Mooney-Rivlin equation. The results showed that, the stress values depend upon pores distribution mode, as the elongation ratio is the same. In all investigated elongation ratio cases the lowest stress forms in such elastomeric material that exhibit the lowest stiffness changes of matrix adjacent zones.

If at low elongation ratio values ($\lambda < 1.4$) the principal stresses of porous elastomeric polymer material are similar to those of non-porous material with the same mechanical properties as the matrix, at high elongation ratio ($\lambda > 1.4$) the principal stresses of porous material are 1.5 – 3 times higher than those of non-porous one.

The results of experimental tests provide good agreement with these numerically obtained but the phenomenon of strengthening was observed as the higher stress in microstrips than true stress at fracture of matrix material appears. This can occur if the pores size is on the order of materials dimensions. Due to this, the strengthening effect would not appear in microporous elastomers.

REFERENCES

1. **Huang, Z., M, Ramakrishnab, S., Tay, A., A., O.** Modeling the Stress/Strain Behavior of a Knitted Fabric-Reinforced Elastomer Composite *Composites Science and Technology* 60 2000: pp. 671 – 691.
2. **Brieu, M., Deries, F.** Micro-Mechanical Approach and Algorithm for the Study of Damage Appearance in Elastomer Composites *Composite Structures* 46 1999: pp. 309 – 319.
3. **Kakavas, P. A., Anifantis, N. K**. Effective Moduli of Hyperelastic Porous Media at Large Deformation *Acta Mechanica* 160 2003: pp. 127 – 147.
4. **Gibson, L. J.; Ashby, M. F.** Cellular Solids: Structure and Properties. Cambridge, Cambridge University Press, 1997: 510 p.
5. **Mills N. J.** Micromechanics of Polymeric Foams *Proceedings of 3rd Nordic meeting on Materials and Mechanics, Aalborg, Denmark* 2000: pp. 45 – 76.
6. **Mills, N. J., Fitzgerald, C., Gilchrist, A., Verdejo, R.** Polymer Foams for Personal Protection: Cushions, Shoes and Helmets *Composites Science and Technology* 63 (16) 2003: pp. 2389 – 2400.
7. **Mills, N. J., Gilchrist, A.** Modeling the Indentation of Low Density Polymer Foams *Cellular Polymers* 19 2000: pp. 389 – 412.
8. **Mills, N. J., Zhu, H. X.** The High Strain Compression of Closed - Cell Polymers Foams *Journal of the Mechanics and Physics of Solids* 47 1999: pp. 669 – 695.
9. **Zhu, H. X., Mills, N. J.** Modelling the Creep of Open - Cell Polymer Foams *Journal of the Mechanics and Physics of Solids* 47 (7) 1999: pp. 1437 – 1457.
10. **Lakes, R., Rosakis, P., Ruina, A.** Microbuckling Instability in Elastomeric Cellular Solids *Journal of Materials Science* 28 1993: pp. 4667 – 4672.
11. **Schjodt-Thomsen, J., Pyrz, R.** Stress - Strain Modelling of Micro Cellular Materials *Proceeding of the 3th Nordic Meeting on Materials and Mechanics, Aalborg, Denmark* 2000: pp. 5 – 17.
12. **Danielsson, M., Parks, D. M., Boyce, M. C.** Constitutive Modeling of Porous Hyperelastic Materials *Mechanics of Materials* 36 (4) 2004: pp. 347 – 358.
13. **Everett, R. K., Matic, P., Harvey II, D. P., Kee, A.** The Microstructure and Mechanical Response of Porous Polymers *Materials Science and Engineering A* 249 1998: pp. 7 – 13.
14. **Kouznetsova, V., Brekelmans, W. A. M., Baaijens, F. P.** An Approach to Micro - Macro Modeling of Heterogeneous Materials *Computational Mechanics* 27 (1) 2001: pp. 37 – 48.
15. **Zeleniakiene, D., Kleveckas, T., Liukaitis, J., Fataraite, E.** The influence of Porosity Value and Mode on Soft Materials Behaviour *Materials Science* (*Medžiagotyra*) 9 2003: pp. 201 – 205.
16. **Zeleniakiene, D., Kleveckas, T., Liukaitis, J., Marazas, G.** The Influence of Porosity on Stress and Strain State of Porous Polymer Materials *Materials Science* (*Medžiagotyra*) 9 2003: pp. 358 – 362.
17. **Macosko, Ch. W.** Rheology: Principles, Measurements, and Applications. New York, VCH Publishers, 1993. 550 p.
18. **Nielsen, L. E.; Landel, R. F.** Mechanical Properties of Polymers and Composites. New York, Marcel Dekker 1994. 557 p.
19. **Bicerano, J.** Prediction of Polymer Properties. New York, Marcel Dekker, 2002: 756 p.
20. **Liukaitis, J.** Principles of Polymer Rheology. Kaunas, Technologija, 1999: 106 p. (in Lithuanian).
21. **Andrews, E. W., Gibson, L. J.** The Influence of Cracks-Like Defects on the Tensile Strength of an Open-Cell Aluminum Foam *Scripta Materialia* 44 2001: pp. 1005 – 1010.
22. **Andrews, E. W., Gibson, L. J.** The Influence of Cracks, Notches and Holes on the Tensile Strength of Cellular Solids *Acta Materialia* 49 (15) 2001: pp. 2975 – 2979.
23. **Andrews, E. W., Gibson, L. J.** On Notch - Strengthening and Crack Tip Deformation in Cellular Metals *Materials Letters* 57 (3) 2002: pp. 532 – 536.

DOI: 10.5755/j02.ms.26530